Title

Variation around the Pyramid theme: optical recombination and optimal use of photons

Authors

Fauvarque, Olivier
Neichel, Benoit
Fuso, Thierry
et al.

Peer reviewed

Variation around the Pyramid theme: optical recombination and optimal use of photons

Olivier Fauvarque[a], Benoit Neichel[a], Thierry Fusco[a,b], and Jean-Francois Sauvage[a,b]

[a]Aix Marseille Université, CNRS, LAM (Laboratoire d'Astrophysique de Marseille) UMR 7326, 13388, Marseille, France
[b]ONERA–the French Aerospace Laboratory, F-92322 Châtillon, France

ABSTRACT

We propose a new type of Wave Front Sensor (WFS) derived from the Pyramid WFS (PWFS). This new WFS, called the Flattened Pyramid-WFS (FPWFS), has a reduced Pyramid angle in order to optically overlap the four pupil images into an unique intensity. This map is then used to derive the phase information. In this paper this new WFS is compared to two existing WFSs, namely the PWFS and the Modulated PWFS (MPWFS) following tests about sensitivity, linearity range and low photon flux behavior. The FPWFS turns out to be more linear than a modulated pyramid for the high-spatial order aberrations but it provides an improved sensitivity compared to the non-modulated pyramid. Furthermore, the pixel arrangement being more efficient than for the PWFS, the FPWFS seems particularly well suited for high-contrast applications. A first quick study of the influence of the angle of the pyramid shows that, it is possible, with a quite constant linear range, to adjust the spatial frequencies range where the sensitivity is the best. Finally, we also show that replacing the pyramid with a flattened cone also leads to very promising noise propagation properties.

Keywords: Active or adaptive optics; Turbulence; Wave-front sensing; Telescopes.

1. INTRODUCTION

The aim of a Wave Front Sensor (WFS) is to code the phase information using an incoming photon flux. WFSs are usually divided into two main classes, those working in the pupil plane like e.g. the Shack-Hartmann,[1] and those performing this operation by imaging the pupil after a Fourier filtering in the focal plane. The Foucault's knife (see Wilson et al.[2]) is a first example of this latter approach. In that case, the focal plane mask is simply an Heaviside function, with half of the light passing through, while the other half is blocked. By re-imaging a pupil plane, one can derive the phase information by analyzing the intensity distribution. This principle has later been generalized by Ragazzonni et al.[3] with the *Pyramid*-WFS (PWFS). In the case of the PWFS the filtering is made by a transparent square pyramid, its summit being positioned on the focal point of the optical system. The prism shape of this optical object spreads the complex amplitude into four parts coding differently the spatial frequencies. The differential information computed from the four resulting intensities allows to easily code the phase information.

2. THE FLATTENED PYRAMID

2.1 Optical design

We propose here a variation around the Pyramid concept, the idea being to recombine the phase information before the detection. To do so, we propose to reduce significantly the pyramid angle so that the four images, which were, in the original concept, completely separated, move closer and overlap. This is illustrated in Fig. 1 where we show three configurations: a full pupil separation (left insert; classical PWFS configuration), a small

Further author information, send correspondence to
Olivier Fauvarque : olivier.fauvarque@lam.fr
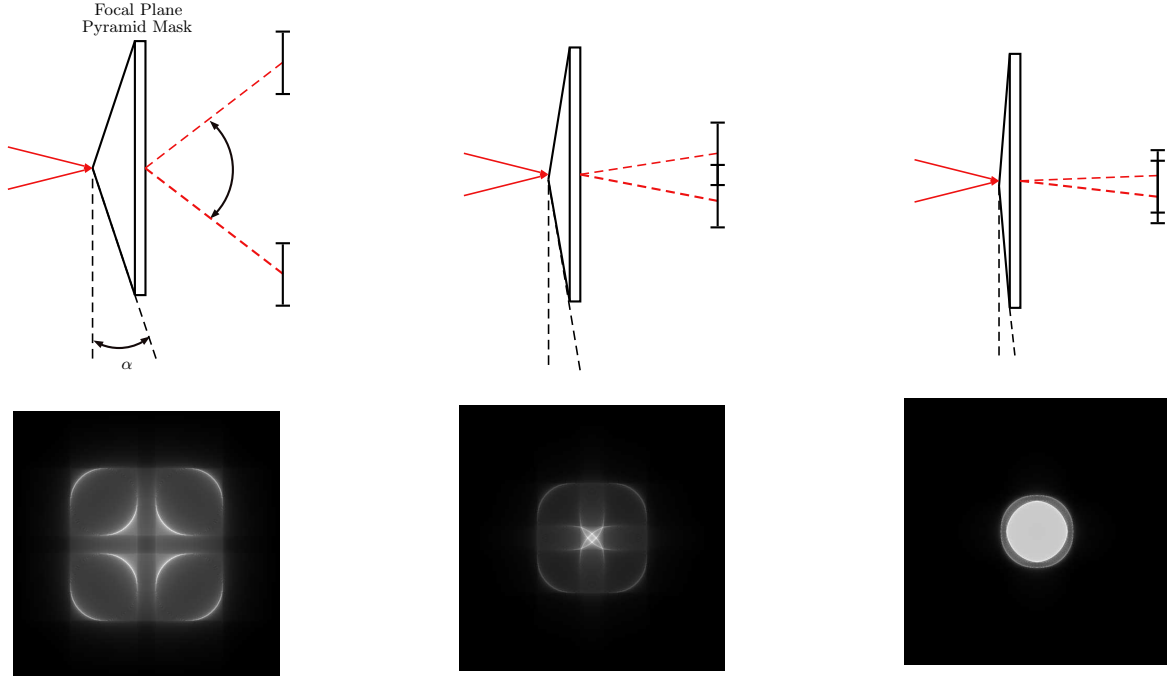Benoit Neichel : benoit.neichel@lam.fr

Figure 1. Schematic optical filtering in the focal plane when the angle of the apex of the pyramid is decreasing. Corresponding intensities on the detector for a flat incoming phase.

overlap (middle insert; overlap rate of 10%) and an overlap rate of 90% (right insert). This resulting intensity distribution can then used as a phase information coding.

The WFS considered here will use a constant overlap rate of 90% (right insert of the figure 1). Due to the shape of the Pyramid, this new WFS will be called FPWFS for Flattened Pyramid Wave Front Sensor.

Note that the influence of the overlap rate parameter is studied in the section 4.

The aim of this letter is to derive the main characteristics of this new WFS in terms of linearity, sensitivity and noise propagation, and to compare them with existing WFSs. To do so, two WFSs have been chosen, respectively:

- the PWFS already introduced above.

- the Modulated PWFS (introduced by Ragazzoni in the same article[3]) which improves the PWFS linearity range, as a trade-off with sensitivity. In this paper, a circular tip/tilt modulation with an amplitude going from 2 to 6 λ/D (in radius) will be considered.

2.2 Definition of the *meta-intensities*

In order to study the performance of a WFS, the first step is to know how to compute the intensity directly coming from the detector to create a quantity (called meta-intensity) which should be linear with the Optical Path Difference (OPD). We assume that the incoming flux is uniform (i.e. we neglect scintillation effects) and defined by

$$\psi = \sqrt{n} P e^{2\iota\pi\frac{\delta}{\lambda}} \tag{1}$$

where ψ is the complex amplitude of the light just in the pupil, n is the number of incoming photons in the full pupil, P is the indicator function of the pupil which informs about the geometry of the pupil and δ is the OPD of the incoming light. The aim of any WFS is to measure this latter quantity. The intensity on the detector $I(\delta, n)$ depends on the OPD and is proportional to the flux.

In the case of the PWFS and the MPWFS, the meta-intensities usually defined (see Ragazzoni in[3]) are the classical *slopes* maps S_x and S_y defined by:

$$S_x = \frac{I_1 + I_2 - I_3 - I_4}{I_1 + I_2 + I_3 + I_4} \quad \text{and} \quad S_y = \frac{I_3 + I_2 - I_1 - I_4}{I_1 + I_2 + I_3 + I_4} \tag{2}$$

where I_1, I_2, I_3 and I_4 are the intensity in the 4 pupil images. Note that this meta-intensities could be chosen differently, see Vérinaud.[4] Only the photons inside the geometrical pupil footprint are taken into account. This is illustrated by the interest area shown in the bottom left and middle insert of the figure 2.
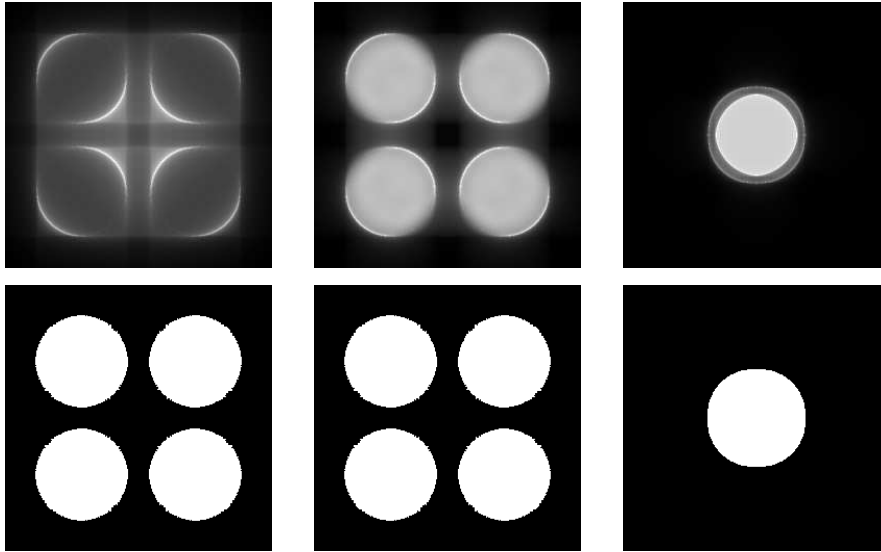

Figure 2. **Intensity** on the detector for a flat incoming phase and **Interest Area** for the **Pyramid WFS**, the **MPWFS** and the **Flattened PWFS**. Note the non-circular shape of the Flattened Pyramid's interest area.

Concerning, the FPWFS, the chosen meta-intensity consists in a return-to-reference and a normalization:

$$mI(\delta) = \frac{I(\delta, n)}{n} - \frac{I(ref, m)}{m} \tag{3}$$

$I(ref, m)$ is the intensity on the detector when the optical aberration corresponds to the reference phase with a reference incoming flux m. Such a meta-intensity, although basic, is the simplest way to recode the intensity and can be used for every WFS which optically codes the phase into intensity. In our case, the reference phase is the zero-OPD but in practice, it may contain WFS path aberrations. In addition, and in order to follow the same computation as for the PWFS, photons which are diffracted outside the geometrical footprint of the pupil on the detector are removed from computation. For the FPWFS, it corresponds to the pupils overlap area, illustrated by the bottom right insert of the figure 2.

3. PERFORMANCE CRITERIA

3.1 Photon management

This first performance paragraph will asses the behavior of the different WFSs in terms of **photon management**, i.e. the way each WFS is managing and optimizing each incoming photon with respect to each detector pixel. Note that this issue is central for low photon flux regimes which is usually the case for astronomical applications.

A first approach to evaluate the WFS efficiency in dealing with low flux regimes is simply to evaluate how many photons are lost by the diffraction and the windowing. Table 1 shows these quantities. The PWFS only uses about 45% of the incoming photons. This is due to the diffraction which rejects light outside the 4 pupils images, especially in the cross area between these images (see the top left insert of the figure 2). The modulation

corrects this by moving back the photons into the 4 pupil images with an efficiency of approximately 90% (see the top middle insert of the figure 2). This value slowly increases with the amplitude modulation. In comparison, the FPWFS makes a better use of the incoming photons, with ∼98% of them effectively used. This is the consequence of having removed the pupil separation.

Table 1. Efficiency of photons.

WFS	P	$\mathrm{MP}_{3\lambda/D}$	FP
Percentage of used photons	43	88	**98**

Secondly, the optical recombination of the 4 pupil signals operated in the FPWFS, requiring a smallest area on the detector compared to the PWFS, tends to prove that the FPWFS is particularly adapted to low photon flux regime. Indeed, for a same pupil sampling, 4 pixels are needed for the PWFS whereas only 1.1 is required for the FPWFS (for a 90% overlap rate). As a consequence, the averaged flux per pixel will be about four times higher in the case of the FPWFS. This may be very interesting if the detector presents significant electronic noise as it is the case for the near IR detectors. Furthermore, for a WFS working at a visible wavelength – where today detectors have sub-electronic noise – the fact that the FPWFS needs less pixels than the PWFS may still be interesting. Indeed, in the context of Extreme AO (XAO), where a very large number of aberrations modes have to be mesured, a smaller detector can be very welcome since costs and data processing speed will be improved.

3.2 Sensitivity

In this second *performance test* paragraph, we will focus on the **sensitivity** of the FPWFS in terms of noise propagation. Following the results of Rigaut and Gendron,[5] the diagonal elements of $(M^t M)^{-1}$, where M is the interaction matrix of the system, have to be studied. The interaction matrix is defined on the first 24 Zernike radial orders which corresponds to the first 299 Zernike modes. Each mode has the same amplitude: 10 nm RMS at λ=630 nm (which corresponds to a 0.1 rad RMS phase amplitude). Moreover, we will use a very high number of pixels on the detector (i.e. 4096) so that any effects of pupil sampling on the noise propagation coefficients, i.e. aliasing effects, can be neglected. For each WFS case, the interaction matrix is built with the meta intensities defined above (S_x and S_y for the PWFS and the MPWFS; mI for the FPWFS and the ZWFS).

Fig. 3 shows the diagonal elements of $(M^t M)^{-1}$ averaged for each Zernike radial order.

In terms of noise propagation, the PWFS presents a very good performance, with a flat distribution of the errors across the Zernike modes, attesting its well known "phase sensor behavior". The modulation increases the value of the noise propagation coefficients for higher frequencies up to five times the PWFS one. Modulation also changes the slope for lower frequencies showing a "slope sensor behavior". This is in good agreement with the findings of Verinaud[4] and Guyon.[6] In comparison, the FPWFS has a very interesting behavior, with a noise propagation close to the MPWFS (modulation of 1.5 λ/D) for low order Zernikes (up to a radial order of ∼4), and then an improved performance when compared to the PWFS itself. Finally, the noise propagation performance of the FPWFS is at least 10 times better (which corresponds to a magnitude gain of 2.5) than the MPWFS modulated at 6 λ/D which is the typical operating modulation amplitude.

These results are confirmed with regard to the cumulated noise in the table 2. Note that the PWFS cumlated noise is chosen as the reference.

Table 2. Cumulated noise normalized to one of the pyramid.

WFS	P	$\mathrm{MP}_{2\lambda/D}$	$\mathrm{MP}_{3\lambda/D}$	$\mathrm{MP}_{6\lambda/D}$	FP
Cumulated noise	1.00	4.01	5.71	15.9	0.64

3.3 Linear range

The following paragraph is focused on the **linearity range** of the FPWFS when compared to the other WFSs. The numerical simulations performed here test the validity of the interaction matrix of each WFS when the aberration amplitude is not equal to the calibration amplitude (here equal to 10 nm RMS at λ=630 nm). To do this, for each Zernike mode, an aberration with an increasing amplitude is sent to the WFSs. The outgoing
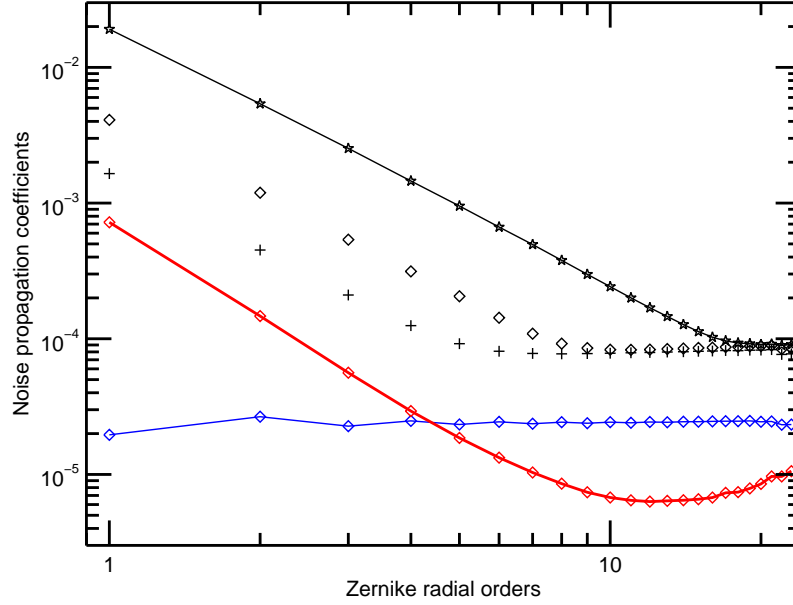
Figure 3. Noise propagation of the **FPWFS** (red), the **PWFS** (blue) and the **MPWFS** (black: $\star_{6\lambda/D}$, $\diamond_3$ and $+_2$).

meta-intensity is inverted via the pseudo-inverse of the interaction matrix. The linearity range associated to this mode is defined as the amplitude where the error between the estimated and the injected amplitude reaches 5 nm RMS. This is shown in Fig. 4 for the 24 first Zernike radial orders.

As already demonstrated in previous studies (Burvall et al. in the article[7]), the PWFS has a low level of linearity range for all considered modes. This level stays quite flat and slowly decreases with the radial order. The FPWFS has the same type of flat linearity range. Nevertheless, the FPWFS is better than the two others since its mean linearity range stays around 50 nm RMS compared to 30 nm for the PWFS.

Concerning the MPWFS, the tip/tilt modulation releases, as expected, the linearity limitation of the PWFS, especially for the low frequencies. Unfortunately, this gain dramatically drops for the high radial orders. As a consequence the FPWFS becomes better from a certain radial order: for a modulation of $1\lambda/D$, this order equals to 3, for $3\lambda/D$ it equals to 7 and for a modulation of $6\lambda/D$ the radial order of equivalent linearity range between the FPWFS and the MPWFS equals to 17.

In the context of Extreme Adaptive Optics, this result could imply that the FPWFS may not need modulation device.

The previous study was only interested in the linearity range regarding isolated aberrations. But the WFSs have to analyze real turbulent phase screens which correspond to a sum of many aberrations. In order to know how each WFS behaves regarding this coupling of several aberrations modes, the *bootstrap* test consists in trying to close an adaptive optics loop when a typical turbulence screen is injected in the Adaptive Optics (AO) system. First simulations show that the MPWFS does manage to close the loop and is the fastest WFS. Despite its low linearity range, the PWFS turns out to bootstrap effectively. Concerning the FPWFS, it does converge and is as fast as the PWFS. These preliminary results are very encouraging with regards to the robustness of the FPWFS, a property that is extremely important in adaptive optics.
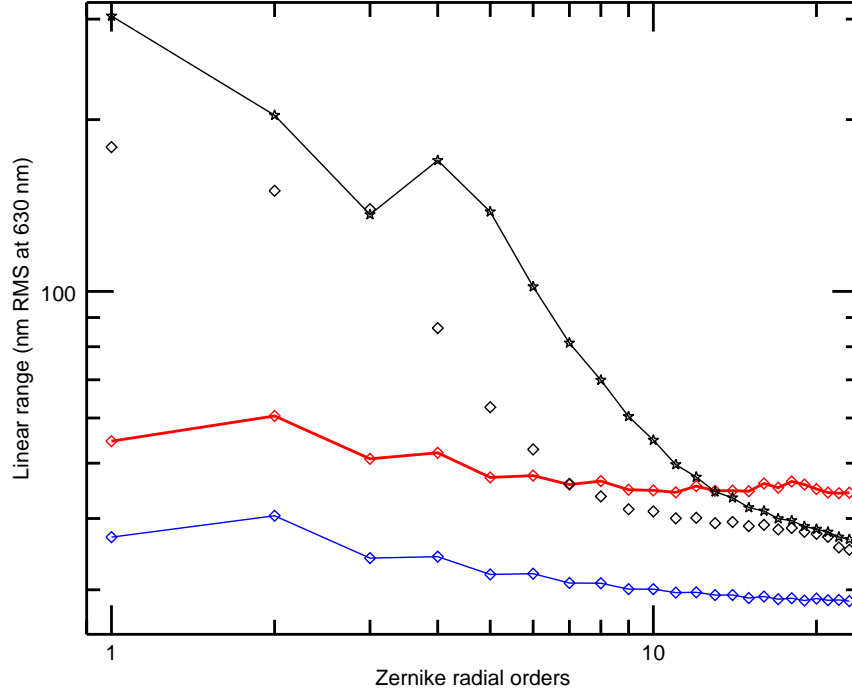
Figure 4. Linearity range of the **FPWFS** (red), the **PWFS** (blue) and the **MPWFS** (black: $\star_{6\lambda/D}$ and $\diamond_3$).

4. INFLUENCE OF THE OVERLAP RATE OF THE PUPILS ON THE PERFORMANCE CRITERIA

In this section, we explore the dependence of the sensitivity and the linear range of the FPWFS when the angle, and subsequently the overlap rate of the pupils, changes. Three configurations are studied from an overlap rate of 75% to 95% (see the intensity for a flat incoming phase on the figure 5).
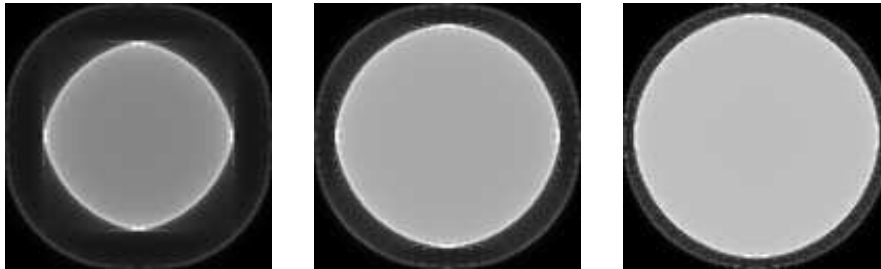

Figure 5. Intensity on the detector for a flat phase for the FPWFS (left insert: overlap rate of the pupils of 75%, middle insert 90% and left insert:95%)

The left graph of the figure 6 shows the dependence of the noise propagation curves with regard to the angle of the apex Pyramid. It appears that the sensitivity increases for the low spatial frequencies when the angle becomes smaller. Nevertheless, the maximum of the sensitivity moves toward the high spatial frequencies as the overlap rate of the pupils decreases.

In terms of linear range, the right graph of the figure 6 shows that there is not a large dependence of the linear range regarding the overlap rate.

Subsequently, it means that if we consider the Fourier filtering mask inserted on the focal plane as an
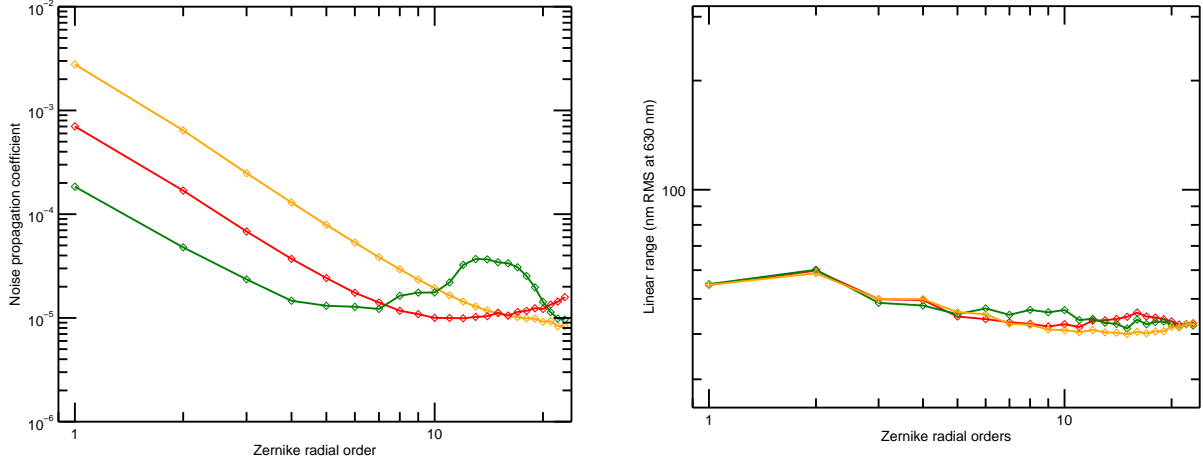
Figure 6. Noise propagation (left graph) and Linear range (right graph) of the **FPWFS** for different overlap rate of the pupils: 75% (green cruve), 90% (red) and 95% (orange)

adjustable element of the wave front sensing path, it would be possible to correct very efficiently a chosen and specific range of the spatial frequencies of the incoming phase by changing the angle of the pyramid.

5. CONCLUSIONS

A new WFS has been derived using the same optical design as the Pyramid WFS. The only modification is to consider a smaller Pyramid angle in order to let the pupil signals overlap. It allows an optical recombination of the four pupil images directly on the detector.

The new Flattened Pyramid WFS presents extremely promising performance. It appears in particular that this sensor conciliates two pillars of WFS: the sensitivity and the linearity range. More specifically, we demonstrated on simulations that:

- At low radial orders (typically <4), the FPWFS provides the same noise propagation performance as a PWFS modulated with an amplitude of about 1.5 λ/D. At high radial orders, its behavior is strongly improved with almost a gain of one order of magnitude with respect to the PWFS.

- The linearity range of the FPWFS outperforms compared to other static WFSs as the PWFS. And even if the FPWFS is not as effective as a large modulated MPWFS for the first Zernike radial orders, it becomes more linear for higher modes. It means that the FPWFS may not require any modulation.

- We tested how the FPWFS could behave regarding real turbulence screens. As for the pyramid, and even if the linearity range is not as good as for other sensors, the FPWFS can effectively and efficiently close an AO loop.

- Diffraction effects are reduced and photons which were lost between the pupil images for PWFS (and to a lesser extent for MPWFS) are now used to code phase information.

- The illuminated area on the detector is smaller for the FPWFS than for the PWFSs. As a consequence, the new sensor requires less pixels to measure a same number of aberrations, what makes of it a WFS particularly appropriate to high-contrast applications.

- A study of the angle parameter influence shows that the linear range does not change with the apex angle whereas it allows to choose the spatial frequencies range where the sensitivity is the best.

APPENDIX A. THE FLATTENED CONE

In this appendix, we study the performance of a new WFS using, instead of a flattened Pyramid, a flattened Cone deployed on the focal plane of the WFS. The idea of using an axicon as a Fourier filtering mask was introduced by Vohnsen et al.[8] but we choose here to explore the case of an axicon with a very small angle of its apex. We naturally call this new WFS, the Flattened Cone WFS (FCWFS) and we use here the same definition of the meta-intensities as for the FPWFS (see equation 2).
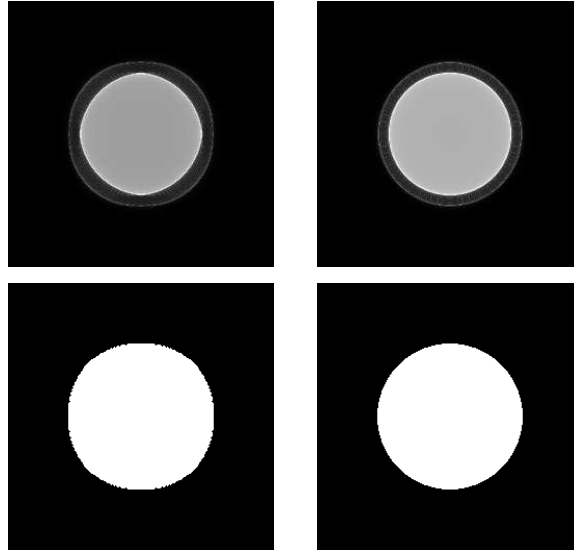

Figure 7. **Intensity** on the detector for a flat incoming phase and **Interest Area** for the Flattened PWFS (left inserts) and the Flattened Cone WFS (right inserts). Note this time the **circular shape** of the Flattened Cone's interest area.

Figure 7 gives a first idea about the behavior of the FCWFS. Indeed, due the great similarity of the intensity for a flat incoming phase with the FPWFS, we except that the FPWFS and the FCWFS have very similar performance. This fact is perfectly verified as regards their sensibility (see the left graph of the figure 8). Concerning the linear range, it appears that the Flattened Pyramid is slightly better than the Flattened Cone (see the right graph of the figure 8). This physical result is quite surprising since we usually think that sensitivity and linearity are antagonist quantities. It could mean that the number of the faces of the "pyramidal" mask (4 for the FPWFS and an infinity for the FCWFS) does matter for the wave front sensing.

ACKNOWLEDGMENTS

REFERENCES

[1] Shack, R. B. and Platt, B. C., "Production and use of a lenticular hartmann screen," *J. Opt. Soc. Am.* **61**, 656 (1971).

[2] Wilson, R. G., "Wavefront-error evaluation by mathematical analysis of experimental Foucault-test data," *Appl. Opt* **14**, 2286–2297 (Sept. 1975).

[3] Ragazzoni, R., "Pupil plane wavefront sensing with an oscillating prism," *Journal of Modern Optics* **43**, 289–293 (Feb. 1996).

[4] Vérinaud, C., "On the nature of the measurements provided by a pyramid wave-front sensor," *Optics Communications* **233**, 27–38 (Mar. 2004).
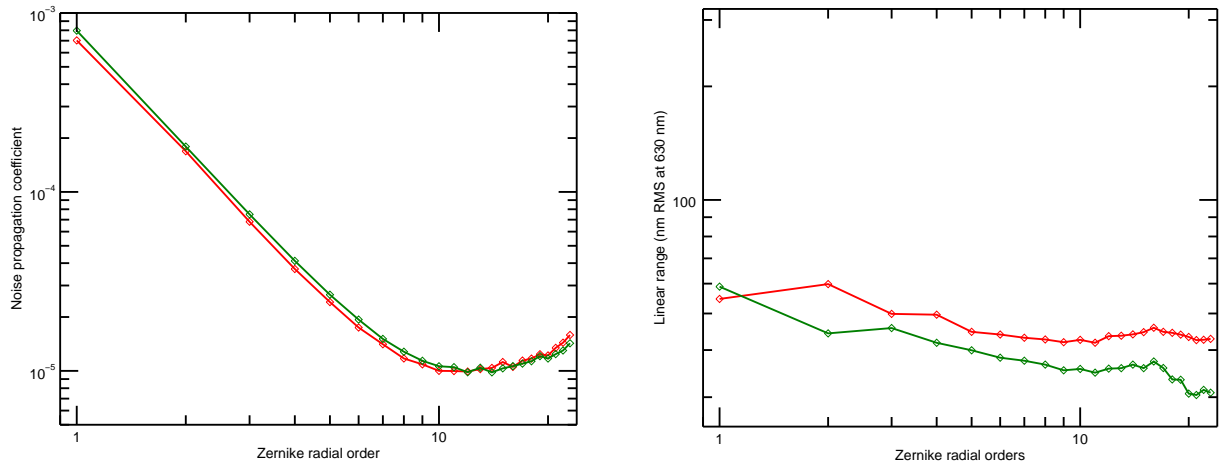
Figure 8. Noise propagation (left graph) and linear range (right graph) for the **FPWFS** (red) and the **FCWFS** (green) for a same overlap rate of the pupils (90%).

[5] Rigaut, F. and Gendron, E., "Laser guide star in adaptive optics. The tilt determination problem," *Astron. Astrophys.* **261**, 677–684 (Aug. 1992).

[6] Guyon, O., "Limits of Adaptive Optics for High-Contrast Imaging," *Astrophys. J.* **629**, 592–614 (Aug. 2005).

[7] Burvall, A., Daly, E., Chamot, S. R., and Dainty, C., "Linearity of the pyramid wavefront sensor," *Optics Express* **14**, 11925–11934 (Dec. 2006).

[8] Vohnsen, B., Castillo, S., and Rativa, D., "Wavefront sensing with an axicon," *Optics Letters* **36**, 846 (Mar. 2011).